NUCLEATION OF SOOT: MOLECULAR DYNAMICS SIMULATIONS OF PYRENE DIMERIZATION

CHARLES A. SCHUETZ AND MICHAEL FRENKLACH

*Department of Mechanical Engineering, University of California, and
Environmental Energy Technologies Division, Lawrence Berkeley National Laboratory,
Berkeley, CA 94720, USA*

Corresponding author: Professor Michael Frenklach
Department of Mechanical Engineering
University of California at Berkeley
Berkeley, CA 94720-1740, USA
Phone: (510) 643-1676
Fax: (510) 642-5539
E-mail: myf@me.berkeley.edu

WORD COUNT

Text (counted by MS Word 2000)	3465
References (7 words × 55 lines)	385
2 Equations (21 words each)	42
Figures (1-200, 2-200, 3-800, 4-200)	1400
1 Table	200
Abstract (not included in Total)	223
Total	5492

Colloquium: **2. Pollutant Formation and Control** (*Subject*: **Soot, PAH**)

Abstract

     Experimental and numerical studies indicate that particle coagulation plays an important role in soot formation. However, to date, neither method has been able to conclusively determine the stage at which chemical precursors begin to coalesce. In the present study, molecular dynamics with "on-the-fly" quantum forces was used to investigate binary collisions between pyrene molecules. The molecular structure and internal motion were treated explicitly. Most of the runs were performed at 1600 K, within the temperature window of soot nucleation in flames. The MD simulations were successful in producing dimers with substantial collisional frequency and lifetimes far exceeding the equilibrium-based predictions, demonstrating that pyrene dimerization is physically realistic in flame environments. The principal finding of the present study is the development of internal rotors by colliding pyrene molecules, the phenomenon responsible for stabilization of the forming dimer. Analysis of the MD results shows that the mechanism of stabilization is rooted in the pattern of energy transfer. The translational energy of the individual colliding molecules is "trapped" in internal rotors that emerge upon collision, and in the vibrational modes of the dimer, including the van der Waals bond established between the pyrene molecules. This model extends the view of stabilization of aromatic species dimerization, with the implication that aromatic dimers of species as small as pyrene can survive long enough to evolve into soot nuclei.

Introduction

Particle inception is the least understood process of soot formation in hydrocarbon combustion. It is widely accepted that gaseous precursors to solid soot particles are polycyclic aromatic hydrocarbons (PAH) [1-6]. However, the understanding of this transformation in mechanistic terms is far from complete.

One may consider the initial phase of the nuclei formation as *purely chemical* growth: aromatic precursors grow in size due to chemical reactions, and, by the virtue of the increasing size, the species acquire the property of a condensed phase. This point of view has received support in several recent studies [7-13]. A purely chemical growth model, tested in numerical simulations, was shown to be able to predict the correct order of magnitude of the incipient soot particle concentration [9,14], but was found insufficient to reproduce the particle size [15]. Detailed modeling demonstrated that the correct magnitude of the particle size requires introduction of particle coagulation, beginning with coalescence of aromatic species [15].

From experimental observations, it is well established that particle coagulation plays an important role in soot formation [1,4,16]. It is thus obvious that regardless of the origin of chemical precursors, sooner or later they begin to coalesce. The question is, at what stage does the coagulation commence, and what form does it take? The majority of numerical studies performed with detailed models of soot formation (see [17-24] and references therein) invoked irreversible dimerization of pyrene molecules as the initial nucleation step for the condensed phase (although smaller [25-27] and larger [28] aromatic species were also employed). From the agreement attained between modeling [6] and experiment—spanning over various properties of soot appearance in laminar premixed [18,29,30], laminar diffusion [21,22,26], and turbulent [19] flames along with stirred-jet [31] and diesel-engine [23,32] combustion—one can conclude that

physical coalescence of PAHs starting at the size of four rings seems to be adequate to explain soot inception in quantitative terms. But is pyrene dimerization at flame conditions physically realistic? Investigation into this question constitutes the subject of the present study.

The choice of pyrene dimerization for initiating particle nucleation was motivated by the exceptional thermodynamic and kinetic stability of this molecule: in a long chain of tightly balanced reversible reactions building aromatic species, pyrene is the first major "island of stability" [14]. However, the assumption of irreversible dimerization of pyrene is in conflict with the results of Miller *et al.* [33]. These authors calculated equilibrium concentrations of benzene, coronene and circumcoronene dimers and found that the estimated values are significantly below the number densities observed for small soot particles in flames. Based on this analysis, they ruled out the possibility that soot nucleation can begin with PAH dimerization. In a follow-up study, Miller [34] calculated size-dependent lifetimes of PAH dimers and found that they approach chemical-reaction times of aromatic growth at a PAH monomer mass four times that of pyrene. In his analysis, Miller [34] relied on the equilibrium results of the prior study [33], but derived PAH collision rates using trajectory calculations. He found that when the relative kinetic energy of the colliding molecules is of the same order as the potential energy well, the molecules can orbit one another for more than 75 ps. However, Miller's findings precluded PAH dimers with mass of less than 800 amu from having lifetimes long enough to contribute to soot nucleation.

In the trajectory calculations of Miller [34], the PAH molecules were assumed to be structureless balls, attracted to each other through the Lennard-Jones potential. In the present study, we investigate binary collisions between pyrene molecules, considering the molecular structure and internal molecular motions, using a technique of molecular dynamics (MD) with

quantum forces that are computed "on-the-fly" [35]. This method allows us to examine, in a more physically realistic way, the dynamics of energy transfer between external and internal degrees of freedom. We chose to focus first on pyrene, due to its presumed role in the kinetic simulations and the "overlap" with the work of Miller and co-workers [33,34]. The principal finding of the performed numerical simulations is that the constituent PAH monomers of the dimer develop internal free rotors, and this phenomenon translates into substantially increased dimer lifetimes.

Theoretical Approach and Computational Procedures

Molecular Dynamics with On-the-Fly Quantum Forces

Molecular dynamics is the technique of modeling the behavior of molecules as a classical system of particles, where the particles are the constituent atoms. A potential function is used to determine the interatomic forces at an instant in time. The motion of the atoms is then determined by numerically integrating differential equations expressing Newton's second law. The numerical integration is repeated over a large number of time-steps, resulting in the evolution of the system over a period of time.

In the present study, the semiempirical PM3 Hamiltonian [36] was used as the interatomic multi-body potential. PM3 is a member of the MNDO family of semiempirical quantum mechanical methods. Semiempirical methods are quantum mechanical in nature, yet they differ from *ab initio* techniques in that some of the computationally intensive terms of the Hamiltonian are replaced with parameters fitted to reproduce experimental data. Semiempirical potentials are thus computationally much faster than *ab initio* ones and hence suitable for use in MD. Additionally, semiempirical potentials are preferable to empirical potentials because they

are quantum mechanical model chemistries and as such should represent atomic interactions more realistically than empirical force fields.

The PM3 Hamiltonian does not explicitly include dispersion, yet it is parameterized to predict the existence of van der Waals forces. For instance, Stewart [37] showed that PM3 predicts the heat of association for the benzene dimer to be –3.8 kcal/mol. This is in good agreement with the *ab initio* work of Jaffe and Smith [38], who computed a 3.33 kcal/mol binding energy at the MP2/6-311G(2d,2p) level of quantum theory, corrected for basis set superposition error using the counterpoise method. In the present study, the binding energy of the pyrene dimer was found to be 4.69 kcal/mol, as obtained in static calculations with the PM3 Hamiltonian. To our knowledge, no quantum *ab initio* study has been carried out on this dimer, and it is unlikely, even nowadays, to do so at a reliable level of theory. From general considerations, the PM3 prediction appears reasonable because the binding is greater than that of the benzene dimer, showing a moderate increase in binding with the monomer size.

At each time step of MD simulation, self-consistent-field (SCF) convergence of the PM3 wave function was achieved, providing the potential energy and the interatomic forces of the system. The numerical integration was performed using the predictor of Beeman's predictor-corrector method [39]. By using a simulation time-step of 0.5 fs, the total energy of the system was maintained constant to within ~1 kcal/mol per 10 ps of simulation time. Further details of this MD technique can be found in Ref. [35].

Collisions of Aromatic Molecules

Prior to the simulation of a collision, the pyrene molecules were vibrationally equilibrated at the simulation temperature. The molecules were brought to vibrational equilibrium with a 5 ps MD run, during which the atomic velocities were rescaled while the

angular and linear momenta of the molecules were held to zero. The velocities were rescaled using the method of Berendsen *et al.* [40], which couples the MD system to a heat bath. After the vibrational equilibration, the molecules were "relaxed" with a 1 ps simulation, during which there was no manipulation of the atomic velocities. This phase allowed the perturbative effects of velocity rescaling and momenta control to damp out.

Simulation of a collision was initiated by positioning two vibrationally equilibrated, but rotationally cold, molecules 15 to 17 Å apart, and giving them opposite translational velocities that would result in a collision. The molecules were prepared rotationally cold in order to emphasize the development of internal rotations. The observation of internal rotations is a critical aspect of the present study. A collection of obvious collision geometries was investigated, including T-shaped, edge-to-edge, and face-to-face (sandwich). For each of the general geometries, several series of runs were made. The impact parameters were varied from zero to greater than the collision diameter, in increments of ~1 Å. Additionally, the initial orientations of the monomers were iterated with rotations of 30° about all three axes. The initial translational velocities of each molecule were varied from the most probable velocity, v_{mp}, assuming a Maxwell-Boltzmann distribution, to as little as 5 % of v_{mp}.

In our study, the instant of collision was defined as the point when the derivative of the intermolecular separation with time changed sign from negative to positive. This marked the instant at which the molecules stopped approaching one another and began to rebound.

Results and Discussion

The technique of molecular dynamics with quantum forces yields more physically realistic simulations, yet it has a much higher computation cost than simulations with empirical potentials. Consequently, this technique cannot be carried out for long reaction times, nor for a

large number of runs. At present, these limitations prohibit this technique from being used to establish the statistics of collisions, which are required to determine the steric collision factor. In light of this, the objective of the present study was to explore the feasibility of colliding pyrene molecules sticking, and hence we only focused on some selected collision geometries that were most favorable to forming dimers. The majority of the runs were conducted at 1600 K, the temperature of soot nucleation in flames [32]. As a very rough measure, out of about 200 runs at 1600 K, approximately 15 % resulted in dimers, with the majority lasting 2 to 8 ps, and a substantial fraction lasting longer. Below, we examine two of these runs to illustrate the general characteristics observed in our study.

Simulation I

This run began with two pyrene molecules, that were vibrationally equilibrated at 1600 K, with zero angular momenta, and positioned 17 Å apart. The initial translational velocity was supplied at 49 % of v_{mp}. The molecules then collided at a simulation time of 3 ps, and remained bound by van der Waals forces for 17 ps.

When the molecules collided the relative angular momenta of the individual molecules, about their respective mass centers, increased rapidly. This is depicted in Fig. 1, which shows that at 3 ps both molecules abruptly began to rotate about the Y axis, and more gradually began to rotate about the X and Z axes. It is also apparent that the molecules exerted torques on one another, as evidenced by the way the relative angular momentum of each molecule changed in a discontinuous manner with time.

In terms of energy, the two molecules initially had a total of 1.71 kcal/mol of translational kinetic energy and zero rotational kinetic energy, as shown in Fig. 2. There was a peak in the translational energy, around 3 ps in the simulation time, as attractive forces

accelerated the molecules toward one another immediately before the collision. When the molecules collided and become bound, the translational energy decreased, and there was a corresponding increase in the rotational kinetic energy. This indicates that translational energy was transferred to internal rotations on a sub-picosecond timescale. A portion of the translational energy was also transferred to the vibrational mode between the pyrene molecules, as evidenced by an oscillation in their intermolecular separation. As the simulation progressed, the rotational kinetic energy increased. Around 17 ps, the rotational kinetic energy reached 6 kcal/mol, exceeding the static binding energy of the pyrene dimer predicted by PM3. This is a significant amount of rotational energy; for comparison, the equilibrium energy of a single free rotor is 1.6 kcal/mol. Shortly after that, at 19.4 ps, there was a sharp decrease in rotational energy and a corresponding increase in the translational energy. From the center of mass separation, it is clear that at this moment the binding between the molecules was broken.

Simulation II

In this run, also at 1600 K, the molecules were initially separated by 17 Å and each was given an initial translational velocity of 15 % of v_{mp}. After the collision the molecules stayed bound for the remaining 17.5 ps of the simulation and there was no indication of the dimer breaking. A sequence of snapshots from this simulation is depicted in Fig. 3. The first two snapshots show the initial configuration of the simulation and the onset of rotations as the molecules collided. The progression of snapshots from 10 ps onward depicts how the molecules continued to rotate after the dimer was formed. The corresponding translational and rotational energies of the two molecules are shown in Fig. 4. As in simulation I, there was an increase in translational energy as the molecules accelerated toward one another immediately before the

collision, at 7.5 ps. Also, in a similar manner to simulation I, the collision was followed by a notable increase in the rotational energy of the system.

Throughout the simulation, there were closely paired spikes in the translational and rotational energies, as can be seen in Fig. 4. These pairs of spikes indicate that the intermolecular vibrational mode and the internal rotors are coupled to each other. For instance, at 10 ps, immediately after a spike in the rotational energy, there was a spike in the translational energy, indicating the transfer of energy between the two modes. Similarly, around 18 ps there was a spike in the translational energy immediately followed by a spike in the rotational energy. These two examples, of pairs of spikes, seem to indicate that there is no preferred direction in the energy transfer: energy can be transferred from translation to rotation or vise versa. It is also interesting to note that while the total energy of the simulation is constant, the sum of the energy in the translational and rotational modes changes rapidly. This indicates that there exists coupling between the A_4-A_4 bond, the internal rotors, and the interatomic oscillators. In other words, it appears that all of the internal modes of the dimer are coupled to one another, thus enabling rapid accommodation of energy released during the collision.

Simulations at 1200 K

A series of additional MD simulations was performed at 1200 K, with the expectation that the collisions would be "stickier". However, out of approximately 100 runs carried out at this temperature, neither the sticking frequency of colliding pyrene molecules nor the lifetime of the forming dimers was noticeably different from that observed at 1600 K. The longest observed dimer at 1200 K was only 12 ps, as compared to over 17 ps at 1600 K. On the basis of these results, we conjecture that the probability of dimer formation is not nearly as sensitive to vibrational temperature as it is to initial translational velocity or the collision geometry. In fact,

10

at both temperatures variations of just 1 % in the initial translation velocity or 0.5 Å in the initial geometry changed the resulting dimer lifetime by as much as 10 ps. Thus, while vibrational modes aid in energy redistribution during the collision, the probability of sticking is only a weak function of vibrational temperature.

Dimer Lifetimes

As mentioned above, the computational cost of the MD simulations prohibits one from obtaining reaction statistics or carrying the calculations long enough to observe when the dimers fall apart. Nonetheless, rough estimates of dimer lifetimes can be made in the following manner.

For a dimer that does not fall apart within the simulation time, we assume that its internal energy distribution has equilibrated to the extent that the laws of statistical mechanics are applicable. In other words, we consider the reaction

$$A_4 \ + \ A_4 \ \rightleftharpoons \ (A_4)_2 \tag{1}$$

obeying detailed balance. True thermal equilibrium can only be attained after multiple collisions with the bath gas. However, we rationalize the present working assumption by the large number of internal degrees of freedom and the shallow (~5 kcal/mol) potential well of the dimer. The equilibrium constant for this reaction can then be expressed as the ratio of partition functions, $K_1 = q_{\text{dimer}}/q_{\text{pyrene}}^2$. The partition function of the dimer, q_{dimer}, and therefore the equilibrium constant, increases with the number of active internal rotational degrees of freedom. The MD simulations indicate that rotations of the individual pyrene molecules within the forming dimer are activated in all three dimensions. However, the same numerical results show that not all of these internal rotors are activated to the same extent, and one would anticipate that some of these internal rotors would be hindered, due to the geometry of the dimer. In light of this, calculations were performed for a range of internal rotational degrees of freedom. The active rotational

modes were treated as free rotors and the remaining degrees of freedom were treated as harmonic oscillators.

With K_1 evaluated in this manner, the approximate dimer lifetime was determined as the inverse of the reverse rate of (1),

$$\tau = \frac{1}{k_{-1}} = \frac{K_1}{k_1} \quad (2)$$

where k_1 and k_{-1} are the rate coefficients of the forward and reverse directions, respectively, of reaction (1). Since it is not currently feasible to find the rate of dimerization from the statistical sampling of MD simulations, the forward rate was assigned to be the gas-kinetic rate. With the assumptions made, equation (2) gives an upper bound for the dimer lifetime.

The results of these calculations are summarized in Table 1. They show that every additional internal rotational mode increases the dimer lifetime by roughly two orders of magnitude. The predicted lifetime of a dimer with only external rotations is extremely short, just 12 fs. However, the MD simulations produced many dimers that survived for a much longer time, more than 10 ps. Even considering that the steric factor would likely reduce the collision frequency, k_1, by one or possibly two orders of magnitude, the dimer lifetimes observed in the MD simulations are much longer than the ones predicted by a thermodynamic model without internal rotors. This strongly suggests the appearance of internal rotations in PAH dimers.

To serve as a soot nucleus, a pyrene dimer must survive until collisions with surrounding gases ensue. The collision rate of a single dimer with the bath gas molecules, like N_2, at 1600 K is on the order of $1 \times 10^{10} \, P \, s^{-1}$, where P is the gas pressure in atm. Thus, a dimer must survive for about $1 \times 10^{-10}/P$ s before the onset of collisions. At 10 atm, a midrange pressure of Diesel combustion, this amounts to 10 ps, definitely shorter than the duration of the dimers we observed in the MD simulations. Furthermore, according to the results presented in Table 1, the ~10 ps

lifetime can be attained with two free internal rotors. Based on the MD simulations, such an expectation is quite reasonable. For instance, the results depicted in Fig. 1 show that each molecule has significant angular momentum about at least one axis. It is conceivable that the dimer could have up to 5 internal rotational modes, and having at least two is extremely likely. With three internal rotors activated, which is still a distinct possibility, the dimer lifetime approaches the chemical reaction times of aromatics growth [15]. These observations suggest that pyrene dimers can survive long enough to participate in the soot nucleation process.

Conclusions

The results of the molecular dynamics simulations demonstrate that pyrene dimerization is physically realistic in flame environments. The MD simulations were successful in producing dimers with substantial collisional frequency and lifetimes far exceeding the equilibrium-based predictions, sufficient to survive until collisions with the surrounding gas ensue. The principal finding of the present study is the development of internal rotors by colliding pyrene molecules, the phenomenon responsible for stabilization of the forming dimer. Analysis of the MD results shows that the mechanism of stabilization is rooted in the pattern of energy transfer. The translational energy of individual colliding molecules is "trapped" in internal rotors emerging upon collision, and in the vibrational modes of the dimer, including the van der Waals bond established between the pyrene molecules. The present model extends that of Miller [34], who proposed an increased stability of aromatic species dimerization due to the development of an orbiting rotation of one incoming molecule around another. However, considering explicitly the molecular structure and internal motion, with the use of a more realistic, quantum-mechanical potential, the present study, while supporting the general notion of rotational stabilization, revealed the development of internal rotations. As many of the internal rotors are seen to be

activated, emergence of internal rotation represents a further increase in stabilization as compared to a single orbiting rotation. The implication of the increased stability is that aromatic dimers of species as small as pyrene can survive long enough to evolve into soot nuclei. The effects of varying species size is the subject of future investigation.

Acknowledgments

REFERENCES

1. Haynes, B.S., and Wagner, H.G., Prog. Energy Combust. Sci. 7:229 (1981).

2. Homann, K.H., Proc. Combust. Inst. 20:857 (1985).

3. Howard, J.B., Proc. Combust. Inst. 23:1107 (1991).

4. Bockhorn, H., Ed., Soot Formation in Combustion: Mechanisms and Models, Springer-Verlag, Berlin, 1994.

5. Glassman, I., Combustion, Academic, San Diego, CA, 1996.

6. Frenklach, M., Phys. Chem. Chem. Phys. 4:2028 (2002).

7. D'Anna, A., D'Alessio, A., and Minutolo, P., Soot Formation in Combustion: Mechanisms and Models (H. Bockhorn, Ed.) Springer-Verlag, Berlin, 1994, p. 83.

8. Minutolo, P., Gambi, G., and D'Alessio, A., Proc. Combust. Inst. 27:1461 (1998).

9. D'Anna, A., and Violi, A., Proc. Combust. Inst. 27:425 (1998).

10. Sarofim, A.F., Longwell, J.P., Wornat, M.J., and Mukherjee, J., Soot Formation in Combustion (H. Bockhorn, Ed.) Springer-Verlag, Berlin, 1994, p. 485.

11. Violi, A., Sarofim, A.F., and Truong, T.N., Combust. Flame 126:1506 (2001).

12. Dobbins, R.A., and Subramaniasivam, H., Soot Formation in Combustion: Mechanisms and Models (H. Bockhorn, Ed.) Springer-Verlag, Berlin, 1994, p. 290.

13. Dobbins, R.A., Fletcher, R.A., and Chang, H.C., Combust. Flame 115:285 (1998).

14. Frenklach, M., Clary, D.W., Gardiner, W.C., Jr., and Stein, S.E., Proc. Combust. Inst. 20:887 (1985).

15. Frenklach, M., and Wang, H., Proc. Combust. Inst. 23:1559 (1991).

16. Wersborg, B.L., Howard, J.B., and Williams, G.C., Proc. Combust. Inst. 14:929 (1973).

17. Kazakov, A., Wang, H., and Frenklach, M., Combust. Flame 100:111 (1995).

18. Appel, J., Bockhorn, H., and Frenklach, M., Combust. Flame 121:122 (2000).

19. Bai, X.S., Balthasar, M., Mauss, F., and Fuchs, L., Proc. Combust. Inst. 23:1623 (1998).

20. Marquardt, M., Mauss, F., Jungfleisch, B., Suntz, R., and Bockhorn, H., Proc. Combust. Inst. 26:2343 (1996).

21. Balthasar, M., Heyl, A., Mauss, F., Schmitt, F., and Bockhorn, H., Proc. Combust. Inst. 26:2369 (1996).

22. Wang, H., Du, D.X., Sung, C.J., and Law, C.K., Proc. Combust. Inst. 26:2359 (1996).

23. Maly, R.R., Stapf, P., and König, G., The Fourth International Symposium COMODIA, The Japan Society of Mechanical Engineers, Kyoto, Japan, 1998, p. 25.

24. Karlsson, A., Magnusson, I., Balthasar, M., and Mauss, F., SAE Trans. 179 (1998).

25. Colket, M.B., and Hall, R.J., Soot Formation in Combustion: Mechanisms and Models (H. Bockhorn, Ed.) Springer-Verlag, Berlin, 1994, p. 442.

26. Smooke, M.D., McEnally, C.S., Pfefferle, L.D., Hall, R.J., and Colket, M.B., Combust. Flame 117:117 (1999).

27. Lindstedt, P.R., Soot Formation in Combustion: Mechanisms and Models (H. Bockhorn, Ed.) Springer-Verlag, Berlin, 1994, p. 417.

28. Pope, C.J., and Howard, J.B., Aerosol Sci. Technol. 27:73 (1997).

29. Markatou, P., Wang, H., and Frenklach, M., Combust. Flame 93:467 (1993).

30. Mauss, F., and Bockhorn, H., Z. Phys. Chem. 188:45 (1995).

31. Brown, N.J., Revzan, K.L., and Frenklach, M., Proc. Combust. Inst. 27:1573 (1998).

32. Yoshihara, Y., Kazakov, A., Wang, H., and Frenklach, M., Proc. Combust. Inst. 25:941 (1994).

33. Miller, J.H., Smyth, K.C., and Mallard, W.G., Proc. Combust. Inst. 20:1139 (1984).

34. Miller, J.H., Proc. Combust. Inst. 23:91 (1991).

35.   Frenklach, M., and Carmer, C.S., Molecular Dynamics of Clusters, Liquids, and Interfaces (W.L. Hase, Ed.) JAI, Stamford, CT, 1999, p. 27.

36.   Stewart, J.J.P., J. Comput. Chem. 10:209 (1989).

37.   Stewart, J.J.P., J. Comput. Chem. 10:221 (1989).

38.   Jaffe, R., and Grant, D., J. of Chem. Phys. 7:2780 (1996).

39.   Beeman, D., J. Comput. Phys. 20:130 (1976).

40.   Berendsen, H., Postma, J., van Gunsteren, W., DiNola, A., and Haak, J., J. Chem. Phys. 81:3684 (1984).
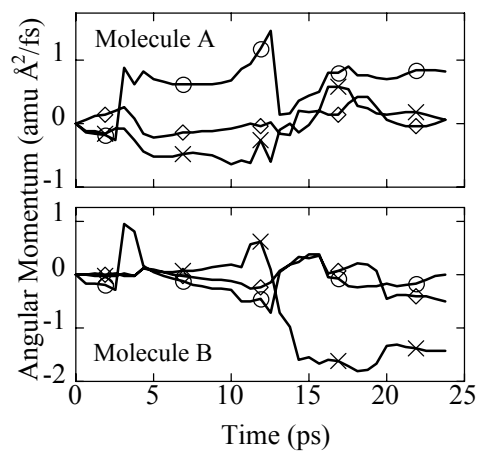
Figure Captions

FIG. 1. The relative angular momenta of the two pyrene molecules in simulation I, about the X (crosses), Y (circles), and Z (diamonds) axes as indicated.   The initial translational velocities of the molecules were along the X axis.

FIG. 2. The translational and rotational kinetic energy of both pyrene molecules in simulation I.

FIG. 3. A series of snapshots from simulation II showing how the monomers develop internal rotations during the formation of a dimer. Shading of the atoms indicates distance from the observer, and arrows indicate the developing rotations.

FIG. 4. The translational (dashed line) and rotational (solid line) kinetic energy of both pyrene molecules in simulation II.

TABLE 1. The dimer lifetimes, calculated according to Eq. 2, for a range of numbers of internal rotational degrees of freedom (IRDF).

IRDF	Lifetime (s)
0	1.2×10^{-14}
1	1.3×10^{-12}
2	5.5×10^{-10}
3	3.0×10^{-7}
4	7.6×10^{-5}
5	4.1×10^{-2}

FIG. 1. The relative angular momenta of the two pyrene molecules in simulation I, about the X (crosses), Y (circles), and Z (diamonds) axes as indicated. The initial translational velocities of the molecules were along the X axis.
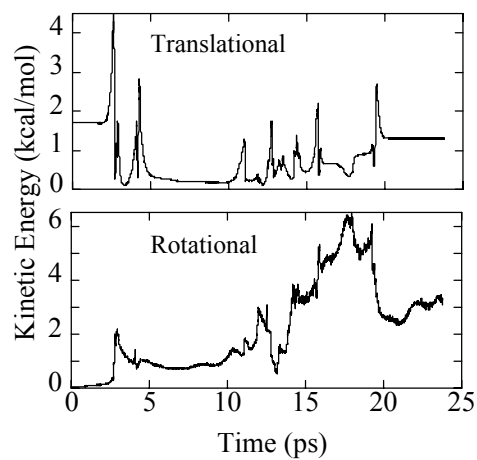

FIG. 2. The translational and rotational kinetic energy of both pyrene molecules in simulation I.
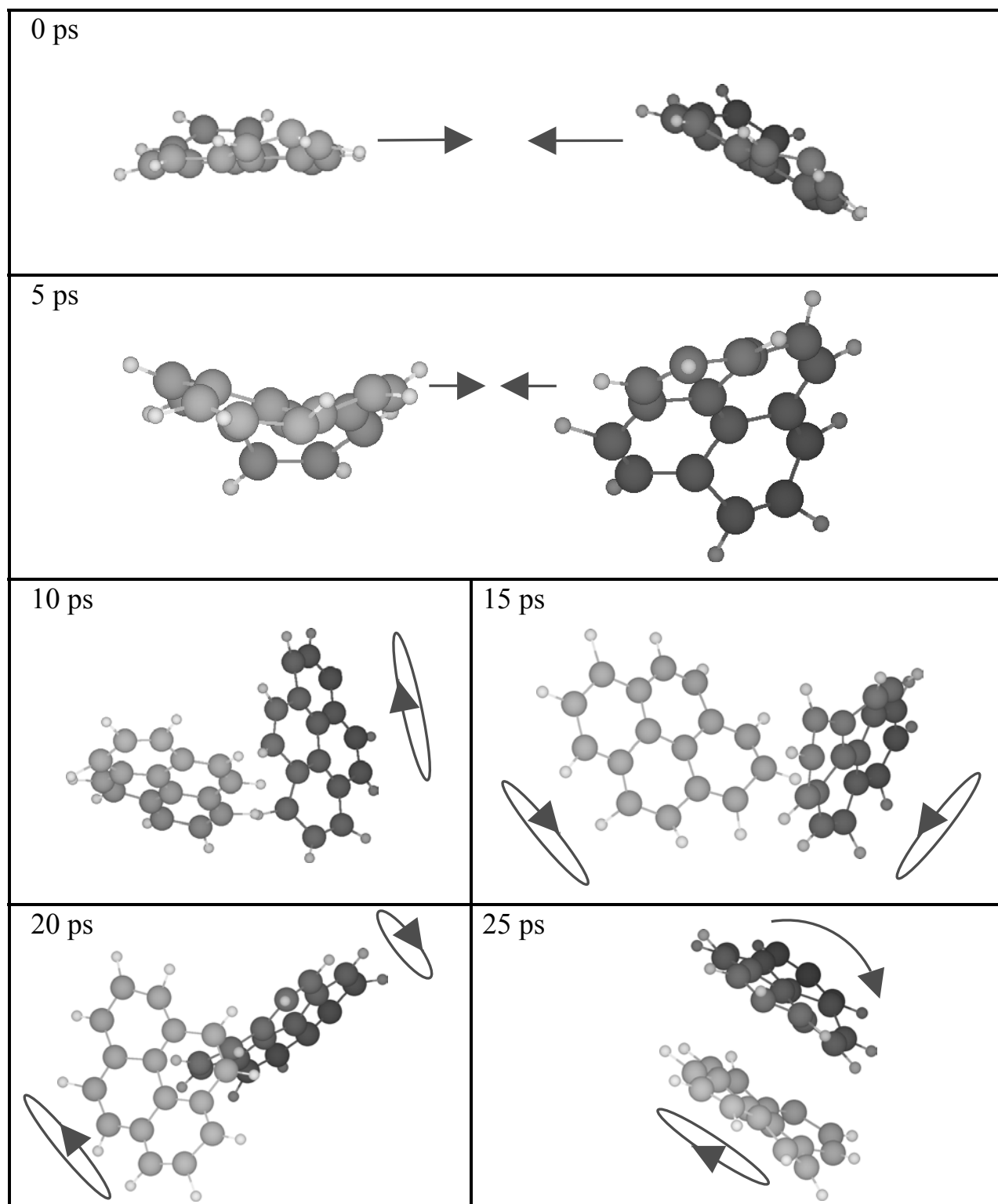
FIG. 3. A series of snapshots from simulation II showing how the monomers develop internal rotations during the formation of a dimer. Shading of the atoms indicates distance from the observer, and arrows indicate the developing rotations.
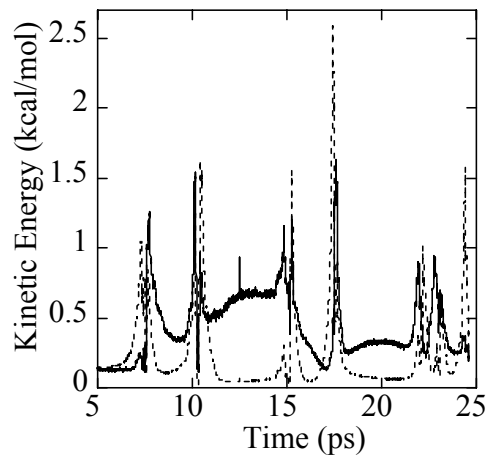
FIG. 4. The translational (dashed line) and rotational (solid line) kinetic energy of both pyrene molecules in simulation II.